Exploring the performances of the dual technique-based water hammer redesign strategy in water supply systems

Mounir Trabelsi and Ali Triki

ABSTRACT

This paper explored and compared the effectiveness of the inline and branching redesign strategies-based dual technique, implemented to enhance the conventional technique skills in terms of attenuation of positive and negative pressure surge magnitudes and limitation of the spreading of pressure wave oscillation period. Basically, this technique is based on splitting the single inline or branched plastic short-section, used in the conventional technique, into a couple of two sub-short-sections made of two distinct plastic material types. Investigations addressed positive and negative surge initiated water hammer events. Additionally, high and low density polyethylene materials were utilized for sub-short-section material. Results illustrated the reliability of the dual technique in protecting hydraulic systems from excessive pressure rise and drop, and evidenced that the (HDPE/LDPE) sub-short-sections' combination (where the former sub-short-section is attached to the sensitive region of the steel piping system parts, while the latter is attached to the second extremity of the steel piping system) is the most prominent configuration providing the best trade-off between pressure surge attenuation, and pressure wave oscillation period spreading. Lastly, it was found that the pressure head peak (or crest) and the pressure wave oscillation period values were markedly sensitive to the (HDPE) sub-short-section length and diameter.

Key words | branching, design, inline, method of characteristics, plastic material, water hammer

Mounir Trabelsi
Department of Mechanics, National Engineering School of Sfax,
University of Sfax,
B. P. 1173, 3038 Sfax,
Tunisia

Mounir Trabelsi
Ali Triki (corresponding author)
Research Unit: Mechanics, Modelling Energy and Materials M2EM, Department of Mechanics, National Engineering School of Gabès,
University of Gabès,
Gabès,
Tunisia
E-mail: *ali.triki@enis.rnu.tn*

INTRODUCTION

Water supply systems are unavoidably subjected to water hammer phenomenon; which is triggered due to either normal setting processes (e.g., opening/closing of valves, starting/stopping of pumps, and variations in in- or out-flow) or accidental events (e.g., improper setting, hydraulic parts or machinery breakdowns). This phenomenon displays a series of positive and negative pressure waves (i.e., unsteady pressure fluctuations), which may be of magnitude large enough to induce severe conditions such as excessive noise, fatigue, stretch or rupture of the pipe wall and even cause major problems potential risky for operators or users (Bergant & Simpson 1999). Consequently, the control of such a transient in pressurized water supply systems constitutes a major concern for designers and pipe system managers to ensure safe and efficient operation, while providing the adequate service level of these utilities.

In this regard, water hammer control strategies typically include: (i) changes within the distribution system (e.g., pipe diameter or profile, wall thickness, alignment and other hydraulic components); (ii) optimization of operational procedures; and (iii) installation of protecting devices at the sensitive locations of the hydraulic system (e.g., automatic control valves, surge tanks, and air chambers) (Wylie & Streeter 1993; Besharat *et al.* 2015; Lamaddalena *et al.* 2018; Wan & Zhang 2018; Deyou *et al.* 2019; Liao *et al.* 2019; Yuzhanin *et al.* 2019). Commonly, a combination of numerous strategies is employed by designers to soften excessive water hammer surges; however, the cumulative effect of

doi: 10.2166/aqua.2019.010

several types of devices may reversely affect water hammer courses, due to substantial inconsistency between the embedded multiple devices (Wylie & Streeter 1993).

Alternatively to classical design measures, recent research entailed novel tools devised upon the ability of polymeric materials to extenuate high- and low-transient pressure (Ferry 1970; Gally *et al.* 1979; Massouh & Comolet 1984; Ghilardi & Paoletti 1986; Pezzinga & Scandura 1995; Triki 2016, 2017, 2018a, 2018b; Triki & Fersi 2018; Fersi & Triki 2019a, 2019b; Trabelsi & Triki 2019; Triki & Chaker 2019). Namely, these studies implemented inline and branching strategies to upgrade or to reconstruct after failure of existing steel pipe-based water supply systems. Specifically, the inline strategy is based on the replacement of a short-section of the sensitive zone of the existing steel piping system by another made of plastic material. The branching strategy is based on adding a branched plastic short-section at the sensitive regions of the original steel piping system. Previous research showed the potential capacity of the inline strategy in attenuating significantly positive and negative water hammer surge magnitudes; however, this strategy induced large spreading of the pressure wave oscillation period. On the contrary, the branching strategy provided important attenuation of pressure head peak and crest, but lower than the inline strategy, and induced a pressure wave oscillation period spreading lower than the inline one. As well, previous work has highlighted that the attenuation of pressure head peak or crest and the spreading of pressure wave oscillation period depend also on the plastic material type employed for the short-section.

Incidentally, the spreading effect of the pressure wave oscillation period may negatively affect the operational procedure of the water supply system, such as increasing the admissible critical time for valve closure (Wylie & Streeter 1993; Triki 2016, 2017, 2018a, 2018b).

Alternatively, to address the foregoing drawback involving the conventional technique-based inline or branching strategy, Triki (2018a, 2018b) and Trabelsi & Triki (2019) proposed a dual technique-based strategy. This technique is based on utilizing an up- and downstream plastic sub-short-section upstream of each of the steel pipe system connections to hydraulic parts. The authors identified that the dual technique allows better trade-off between the attenuation of pressure head and the spreading of pressure wave oscillation period effects than the conventional one.

Accordingly, we planned in the current paper to address further insights for the dual technique concept by comprehensively assessing and comparing the effectiveness of this technique implemented for inline and branching strategies.

In the following section, the methodology followed to estimate the flow parameters is briefly described.

METHODS

For common engineering applications, the one-dimensional (1D) water hammer model combined with the Kelvin–Voigt (Aklonis *et al.* 1972) and the Vitkovsky *et al.* (2000) formulations, can serve as a useful tool for predicting flow parameters involving fast transient events induced into viscoelastic pipes (Wylie & Streeter 1993; Covas *et al.* 2004). This model may be expressed as follows:

$$\frac{\partial H}{\partial t}+\frac{a_0^2}{gA}\frac{\partial Q}{\partial x}+2\frac{a_0^2}{g}\frac{d\varepsilon}{dt}=0 \tag{1}$$

$$\frac{1}{A}\frac{\partial Q}{\partial t}+g\frac{\partial H}{\partial x}+g(h_{f_s}+h_{f_u})=0 \tag{2}$$

where H and Q correspond to the instantaneous pressure head and flow rate; A denotes the cross-sectional area of the pipe; g indicates the gravity acceleration; a_0 designates the wave speed; ε denotes the radial strain; h_{f_s} is the quasi-steady head loss component per unit length determined referring to Colebrook–White ($h_{f_s}=RQ|Q|$) or the Hagen–Poiseille ($h_{f_s}=32\nu'|Q|/(gD^2A)$) rules, for turbulent or laminar flow regimes, respectively; h_{f_u} is the unsteady friction loss approximated according to the Vitkovsky *et al.* (2000) rule ($h_{f_u}=(k_v/gA)\{(\partial Q/\partial t)+a_0\,\mathrm{Sgn}(Q)|\partial Q/\partial x|\}$), where $k_v=0.03$ is the Vitkovsky decay coefficient and $\mathrm{Sgn}(Q)=+1$ or -1 for $Q\geq 0$ or $Q\prec 0$, respectively; x and t denote the coordinates along the pipe axis and time, respectively.

The flow model constitutive equations (Equations (1) and (2)) may be discretized using the method of characteristics (MOC) procedure based on a fixed time step mesh, in order to manipulate multi-pipe systems with different wave speed values.

Briefly, the numerical treatment procedure steps are as follows (further detailed analysis can be found in, for example, Wylie & Streeter 1993).

The compatibility equations associated with the flow model, written in a finite-difference form, are:

$$C^{j\pm}: \frac{dH}{dt} \pm \frac{a_0^j}{gA^j}\frac{dQ}{dt} + \frac{2a_0^2}{g}\left(\frac{\partial \varepsilon}{dt}\right) \pm a_0^j\left(h_{f_s}^j + h_{f_u}^j\right) = 0 \quad \text{along } \frac{\Delta x^j}{\Delta t} = \pm\frac{a_0^j}{c_r^j} \tag{3}$$

where, the superscript j refers to the pipe number ($1 \le j \le np$) and the lower subscript i corresponds to the section index of the j^{th} pipe ($1 \le i \le n_s^j$); n_s^j refers to the number of the j^{th} pipe sections and np stands for the number of pipes; and Δt denotes the time step increment.

The radial strain ε may be estimated using the linear viscoelastic Kelvin–Voigt formulation, for small strains, and assuming homogeneous and isotropic pipe wall material, as follows (Aklonis *et al.* 1972):

$$\varepsilon(x,t) = \sum_{k=1}^{N_{kv}} \varepsilon_k = \sum_{k=1}^{N_{kv}} \rho g \frac{\alpha D}{2e} \int_0^s [H(x,t) - H_0(x)] \frac{J_k}{\tau_k} e^{-\frac{s}{\tau_k}} ds \tag{4}$$

where J_k and τ_k ($k = 0 \cdots n_{kv}$) denote the creep compliance and the retardation time coefficients associated with k^{th} Kelvin–Voigt element, respectively; n_{kv} corresponds to the number of Kelvin–Voigt elements and the indices '0' correspond to the initial steady value.

Hence, the fundamental flow parameters can be straightforwardly computed, in time domain, from Equation (3), yielding:

$$C^{\pm}: \begin{cases} Q_{i,t}^j = c_p^j - c_{a-}^j H_{i,t}^j \\ Q_{i,t}^j = c_n^j + c_{a+}^j H_{i,t}^j \end{cases} \text{along } \frac{\Delta x^j}{\Delta t} = \pm\frac{a_0^j}{c_r^j} \tag{5}$$

where $c_p^j = (Q_{i-1,t-1}^j + (1/B^j) H_{i-1,t-\Delta t}^j + c_{p1}'^j + c_{p1}'''^j)/(1 + c_p'^j + c_{p2}''^j + c_{p2}'''^j)$; $B = a_0/(gA)$; $c_n^j = (Q_{i+1,t-1}^j + (1/B^j)H_{i+1,t-\Delta t}^j + c_{n1}'' + c_{n1}''')/(1 + c_n'^j + c_{n2}''^j)$; $c_{a+}^j = 1 + c_{p2}'''^j/(B^j(1 + c_{p2}'^j + c_{p2}''^j))$; $c_p'^j = R^j \Delta t |Q_{i-1,t-1}^j|$; $c_n'^j = R^j \Delta t |Q_{i+1,t-1}^j|$; $R^j = f^j/2D^jA^j$; $c_{p1}''^j = k_v\theta Q_{i,t-1}^j - k_v(1-\theta)(Q_{i-1,t-1}^j - Q_{i-1,t-2}^j) - k_v \mathrm{Sgn}(Q_{i-1,t-1}^j)(Q_{i,t-1}^j - Q_{i-1,t-1}^j)$; $c_{n1}''^j = k_v\theta Q_{i,t-1}^j - k_v(1-\theta)(Q_{i+1,t-1}^j - Q_{i+1,t-2}^j) - k_v \mathrm{Sgn}(Q_{i+1,t-1}^j)(Q_{i,t-1}^j - Q_{i+1,t-1}^j)$; $c_{p2}''^j = c_{n2}''^j = k_v\theta$; ($\theta = 1$ is a relaxation coefficient); $c_{p1}'''^j = -c_{n1}'''^j = -2a_0^jA^j\Delta t \sum_{k=1}^{n_{kv}} [\varepsilon_k^j(x,t)/\partial t]$; $c_{p2}'''^j = c_{n2}'''^j = 2a_0^jA^jc_0\gamma \sum_{k=1}^{n_{kv}} J_k^j(1 - e^{-(\Delta t/\tau_k)})$; $\varepsilon_{k,i,t-\Delta t}^j = J_k^jc_0\{[H_{i,t-\Delta t}^j - H_{i,0}^j] - e^{-(\Delta t/\tau_k)}[H_{i,t-2\Delta t}^j - H_{i,0}^j] - \tau_k(1 - e^{-(\Delta t/\tau_k)})[H_{i,t-\Delta t}^j - H_{i,t-2\Delta t}^j]/\Delta t\} + e^{-(\Delta t/\tau_k)}\varepsilon_{k,i,t-2\Delta t}$ and $c_0 = \alpha\gamma D^j/2e^j$.

The numerical procedure, outlined above, allows hydraulic parameters' computation, for a single-phase flow. For the cavitating flow onset, the discrete gas cavity model (DGCM) may be included in the (MOC) procedure assuming that cavities are lumped at the computing nodes.

Based on the perfect gas law, the isothermic evolution of each isolated gas cavity can be expressed as:

$$\forall_{g_i}^t (H_i^t - z_i - H_v) = (H_0 - z_0 - H_v)\alpha_0 A \Delta x \tag{6}$$

where H_0 and H_v designate the reference and the gauge pressure head values, respectively; α_0 denotes the void fraction at H_0; and z_i represents the pipe axis elevation.

The equation calculating cavity volume $\forall_{g_i}$, at a given cross section i, is derived from the discretization of local continuity equation using the FG-MOC (Wylie & Streeter 1993):

$$\forall_{g_i}^t = \forall_{g_i}^{t-2\Delta t} + [\psi(Q_{d_i}^t - Q_{u_i}^t) - (1-\psi)Q_{d_i}^{t-2\Delta t} - Q_{u_i}^{t-2\Delta t})]2\Delta t \tag{7}$$

where $\forall_{g_i}$ and $\forall_{g_i}^{t-2\Delta t}$ correspond to the cavity volumes at the current time step and at $2\Delta t$ time steps earlier, respectively; and $0.5 \le \psi \le 1\psi$ is a weighting factor (Bergant & Simpson 1999).

It is worth noting that the cavity collapses inasmuch as $\forall_{g_{i,t}}^j \prec 0$. In this situation, the one-phase water hammer solution (Equation (5)) is valid again.

To achieve the solution at any time step, appropriate boundary conditions should be specified. Specifically, at a junction of a series or branch connection of pipes ($j-1$ and j), the pressure head and the discharge may be evaluated, under the assumptions of no flow storage and a common hydraulic grade-line elevation (Wylie & Streeter 1993):

$$H_{|x=L}^{j-1} = H_{|x=0}^j \text{ and } Q_{|x=L}^{j-1} = Q_{|x=0}^j \text{ for inline connection} \tag{8}$$

$$H^{j-1}_{|x=L} = H^{j}_{|x=0} = H^{d} \text{ and } Q^{j-1}_{|x=L} = Q^{j}_{|x=0} + Q^{d} \text{ for branching connection} \quad (9)$$

where the right and left sides of Equation (8) relate to the hydraulic parameters evaluated at the up- and downstream sides of the junction; and the superscript d corresponds to the branching device parameters.

MODEL VALIDATION

Data from laboratory experiments recorded by Covas *et al.* (2004) are considered to validate the numerical model derived above. The experimental test rig is composed of a single high-density polyethylene (HDPE) pipe (SDR11/PE100/NP16: effective length: $L = 271.8$ m; wall thickness: $e = 6.25$ mm and diameter: $D = 50.6$ mm), an upstream reservoir, and a downstream free discharge valve. The steady-state pressure head at the upstream reservoir and flow rate are set equal to: $Q_0 = 1.008$ l/s and $H_{0|reservoir} = 35$ m, respectively. Results are carried out for a transient flow originating from an abrupt closure of the downstream valve.

Figure 1 illustrates a comparison between measured and computed pressure head signals, obtained by the (1D) unconventional water hammer model versus time. It evidences that the pressure head signals, computed based on the water hammer solver, fit reasonably the measured signals in terms of amplitude and phase shift of pressure head pulses. In addition, the (1D) unconventional water hammer model produces sharp pressure head signals compared with the measured ones. To the authors, this dispersion is mainly due to the viscoelastic pipe wall behavior, rather than to frictional effects.

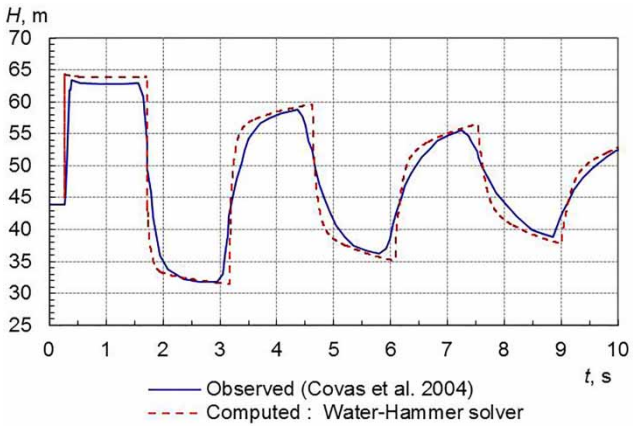

Figure 1 | Comparison between experimental and numerical pressure head traces.

In the following sections, the suggested dual technique is implemented for two case studies involving positive and negative initiated water hammer surges.

APPLICATION SET-UP RESULTS AND DISCUSSION

As mentioned before, the inline or branching design strategy-based dual technique consists of splitting the single inline or ramified plastic short-section used in the conventional technique into a couple of two sub-short-sections made of two distinct plastic material types, placed upstream of each connection of the existing steel pipe to other hydraulic parts. Namely, a {(HDPE) inline (or branched) sub-short-section – steel pipe – (LDPE) inline (or branched) sub-short-section} connections of pipes, denoted henceforward (HDPE/LDPE) inline or branching set-up, respectively, are investigated in the following.

Additionally, for comparison purposes, the results associated with the inline or branching design strategy-based conventional technique are also addressed. Incidentally, the implementation of the conventional technique- based inline or branching strategy corresponds to a {steel pipe inline (or branched) (HDPE) short-section}; and {steel pipe inline (or branched) (LDPE) short-section} connections of pipes, denoted hereinafter (HDPE) inline (or branched) and (LDPE) inline or branching set-ups.

For instance, in order to obtain a consistent comparison with regard to the employed plastic material volume, the (sub-) short-section lengths and diameters, used in each technique, are selected as follows:

$$l^{\text{conventional}}_{\text{short-section}} = 2 \times l^{\text{dual}}_{\text{sub-short-section}} \text{ and } d^{\text{conventional}}_{\text{short-section}} = d^{\text{dual}}_{\text{sub-short-section}} \quad (10)$$

The Kelvin–Voigt characteristics of the employed HDPE or LDPE materials are: $\{J_k[\text{GPa}^{-1}];\ \tau_k[\text{s}]\}^{\text{HDPE}}_{k=0-5} = \{0.8032;\ -/1.057;0.05/1.054;0.5/0.905;1.5/0.262;5/0.746;10\}$ or $\{J_k\ [\text{GPa}^{-1}];\tau_k[\text{s}]\}^{\text{LDPE}}_{k=0-3} = \{\{2.083;-/7.54;0.00089/10.46;\ 0.022/12.37;\ 1.864\}$, respectively (Keramat & Haghighi 2014).

Concerning the MOC algorithm, computations were performed using a specified time step value: $\Delta t = 0.017$ s, a set of Courant number values: $c_r = \{0.9369;\ 0.6758;\ 1\}$, associated with the spatial discretization of the main steel pipe, along with the HDPE and LDPE (sub-) short-sections, respectively, and a weighting factor: $\psi = 0.5$, used for the DGCM procedure.

Case 1: Control of positive-surge initiated water hammer waves

The case study concerns a reservoir steel pipe valve system shown in Figure 2(a). The steel pipe characteristics are: $L = 100$ m; $D = 53.2$ mm; $e = 3.35$ mm; $a_0 = 1369.7$ m/s; and $J_0 = 0.0049$ GPa^{-1}. Initially, the discharge and the downstream pressure head are set at the constant values: $Q_0 = 0.58$l/s and $H_{0|valve} = 45$m, respectively. The transient regime is caused by the sudden and total closure of the downstream valve, initiating a positive surge wave. Thereby, the boundary condition corresponding to such a maneuver may be written as:

$$Q_{|x=L} = 0 \text{ and } H_{|x=0} = H_{0|reservoir}\ (t \succ 0) \tag{11}$$

For such a case, the dual technique-based branching or inline strategy may be implemented as sketched in Figure 2(b) or 2(c).

As a starting step, the inline or branched sub-short-section length and diameter, employed in the dual technique frame, are chosen equal to: $l_{\text{dual}}^{\text{sub short-section}} = 2.5$m and $d_{\text{dual}}^{\text{sub short-section}} (= D) = 53.2$ mm, respectively. Thus, based on the relationship (Equation (10)), the short-section length and diameter, used within the conventional technique frame, are equal to: $l_{\text{conventional}}^{\text{short-section}} (= 2 \times l_{\text{dual}}^{\text{sub short-section}}) = 5$m and $d_{\text{conventional}}^{\text{short-section}} (= d_{\text{dual}}^{\text{sub short-section}}) = 53.2$ mm, respectively.

Figure 3 replicates the comparison between the downstream pressure head signals estimated into the non-protected hydraulic system case and their counterparts involved by the protected system cases implementing the dual or conventional technique based on the inline or branching strategy. Jointly, the main features of the pressure wave pattern, displayed in Figure 3, are reported in Table 1.

First, Figure 3 illustrates that the change in the downstream boundary condition triggered both expansion and compression pressure waves into the original hydraulic system case. In this case, the first positive- or negative-pressure head magnitude is equal to: $\Delta H^+|_{\text{STEEL}} = 40.6$ m or $\Delta H^-|_{\text{STEEL}} = 39.6$ m, respectively; and the period of the first cycle of pressure wave oscillation is equal to: $T_1|_{\text{STEEL}} = 0.42$ s.

Second, Figure 3 exhibits attenuated trends of the pressure head profiles computed into the protected system cases, accompanied with an increase of pressure wave oscillation period value, compared with that predicted in the non-protected system case. Specifically, the extents of the forgoing two effects depend on the employed technique (i.e., dual or conventional) and strategy (i.e., inline or branching).

Specifically, Figure 3 and Table 1 indicate that the first pressure head peak is more attenuated in the case involving the (HDPE/LDPE) branching set-up than that provided by the (HDPE/LDPE) inline set-up ($\Delta H^+|_{\text{HDPE -LDPE}}^{\text{branching}} = 26.6$ m and $\Delta H^+|_{\text{HDPE -LDPE}}^{\text{inline}} = 30.4$ m, respectively). However, referring to Figure 3 and Table 1, the (HDPE/LDPE) branching set-up induces more important spreading of pressure wave oscillation period value than the (HDPE/LDPE) inline set-up ($T_1|_{\text{HDPE -LDPE}}^{\text{branching}} = 0.904$ s and $T_1|_{\text{HDPE -LDPE}}^{\text{inline}} = 0.876$ s). Thereupon, the ratio between the positive-surge magnitude and the period of the first cycle of pressure wave oscillation is: $\{\Delta H^+/T_1\}|_{\text{HDPE -LDPE}}^{\text{branching}} = 29.42$ ms^{-1} or $\{\Delta H^+/T_1\}|_{\text{HDPE -LDPE}}^{\text{inline}} = 34.70$ ms^{-1}, corresponding to the (HDPE/LDPE) branching or inline set-up. In other words, the (HDPE/LDPE) branching set-up offers more important pressure head attenuation and little spreading of pressure wave oscillation period, as compared to the (HDPE/LDPE) inline set-up. From the results' interpretations, it may be concluded that the (HDPE/LDPE) branching set-up leads to better trade-off between pressure head attenuation and wave oscillation period spreading than the (HDPE/LDPE) inline set-up. Consequently, this specific set-up is further interpreted in detail.

As compared with the original system case, the (HDPE/LDPE) branching set-up provides important attenuation of first pressure head peak: $\delta H^+|_{\text{HDPE -LDPE}}^{\text{branching}} = |\Delta H^+|_{\text{HDPE -LDPE}}^{\text{branching}} - \Delta H^+|_{\text{STEEL}}| = 14.0$ m. However, this set-up induces a longer pressure wave oscillation period as compared with the original system case. Specifically, the phase-shift depicted between the (HDPE/LDPE) branching set-up and

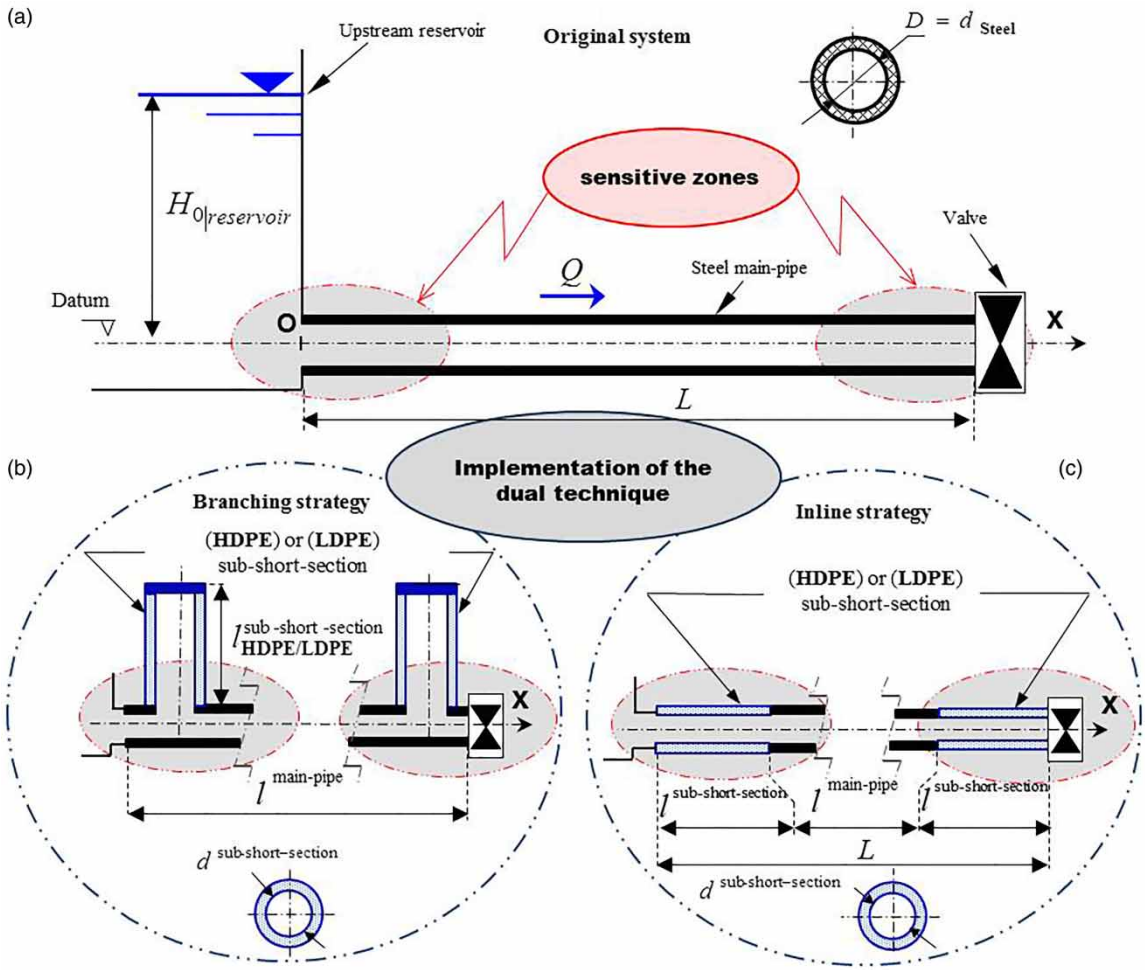

Figure 2 | Sketch of the hydraulic system for the positive-surge control test case: (a) the original system and the controlled system using the dual technique-based (b) branching or (c) inline strategy.

the original system case is equal to: $\delta T_1|^{\text{branching}}_{\text{HDPE}-\text{LDPE}} = |T_1|^{\text{branching}}_{\text{HDPE}-\text{LDPE}} - T_1|_{\text{STEEL}}| = 0.484$ s. In other words, the performance index of the (HDPE/LDPE) branching set-up relatively to the original system case is equal to: $\mu^+|^{\text{branching}}_{\text{HDPE}-\text{LDPE}} = \{\delta H^+|^{\text{branching}}_{\text{HDPE}-\text{LDPE}}/\delta T_1|_{\text{STEEL}}\} = 28.92\,\text{ms}^{-1}$.

Similarly, the (HDPE/LDPE) branching set-up provides more important attenuation of first pressure head peak as compared with the (HDPE) inline or branching set-up: $\delta' H^+|^{\text{branching}}_{\text{HDPE}-\text{LDPE}} = |\Delta H^+|^{\text{branching}}_{\text{HDPE}-\text{LDPE}} - \Delta H^+|^{\text{inline}}_{\text{HDPE}}| = 7.5$ m or $\delta'' H^+|^{\text{branching}}_{\text{HDPE}-\text{LDPE}} = |\Delta H^+|^{\text{branching}}_{\text{HDPE}-\text{LDPE}} - \Delta H^+|^{\text{branching}}_{\text{HDPE}}| = 8.5$ m, respectively. However, the (HDPE/LDPE) branching set-up induces a longer pressure wave oscillation period as compared with the (HDPE) inline or branching set-up. Specifically, the phase shift depicted between the former and latter set-up is equal to: $\delta' T_1|^{\text{branching}}_{\text{HDPE}-\text{LDPE}} = |T_1|^{\text{branching}}_{\text{HDPE}-\text{LDPE}} - T_1|^{\text{inline}}_{\text{HDPE}}| = 0.148$ s or $\delta'' T_1|^{\text{branching}}_{\text{HDPE}-\text{LDPE}} = |T_1|^{\text{branching}}_{\text{HDPE}-\text{LDPE}} - T_1|^{\text{branching}}_{\text{HDPE}}| = 0.156$ s, respectively. In other words, the performance index of the (HDPE/LDPE) branching set-up relative to the (HDPE) inline or branching set-up is equal to: $\mu'^+|^{\text{branching}}_{\text{HDPE}-\text{LDPE}} = \{\delta' H^+|^{\text{branching}}_{\text{HDPE}-\text{LDPE}}/\delta' T_1|^{\text{inline}}_{\text{HDPE}}\} = 50.68\,\text{ms}^{-1}$, or $\mu''^+|^{\text{branching}}_{\text{HDPE}-\text{LDPE}} = \{\delta'' H^+|^{\text{branching}}_{\text{HDPE}-\text{LDPE}}/\delta'' T_1|^{\text{branching}}_{\text{HDPE}}\} = 54.49\,\text{ms}^{-1}$, respectively.

Contrarily, the (HDPE/LDPE) branching set-up provides less important attenuation of first pressure head peak as compared with the (LDPE) inline or branching set-up: $\delta''' H^+|^{\text{branching}}_{\text{HDPE}-\text{LDPE}} = |\Delta H^+|^{\text{branching}}_{\text{HDPE}-\text{LDPE}} - \Delta H^+|^{\text{inline}}_{\text{LDPE}}| = 5.0$ m or $\delta'''' H^+|^{\text{branching}}_{\text{HDPE}-\text{LDPE}} = |\Delta H^+|^{\text{branching}}_{\text{HDPE}-\text{LDPE}} - \Delta H^+|^{\text{branching}}_{\text{LDPE}}| = 4.0$ m, respectively. However, this set-up induces a longer pressure wave oscillation period compared with the (LDPE) inline or branching set-up. Specifically, the phase

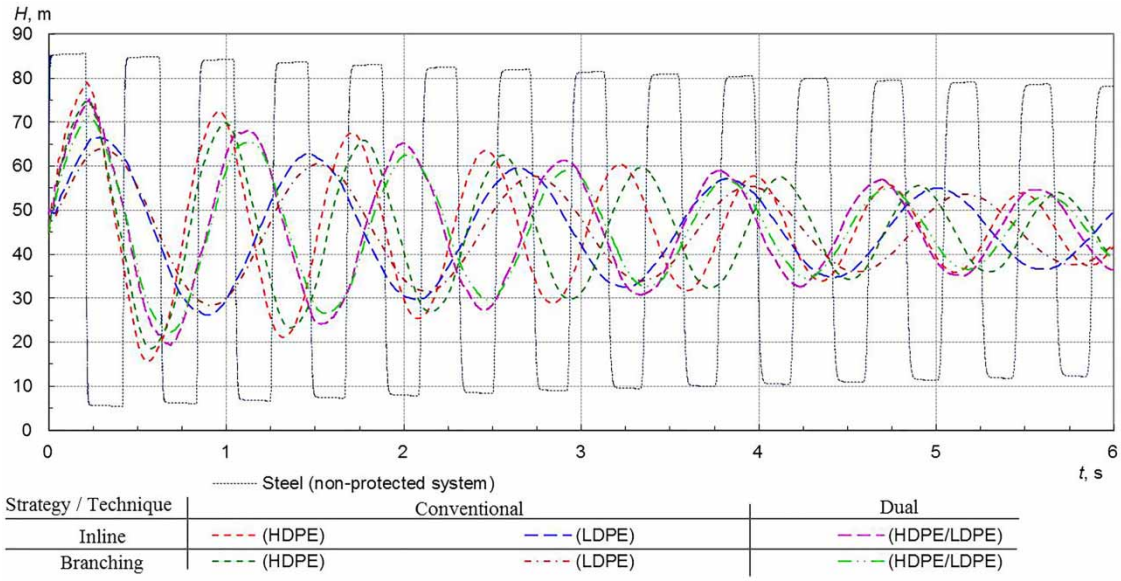

Figure 3 | Downstream pressure head signals, for the non- and protected system cases using the inline or branching strategy based on the dual or conventional technique.

Table 1 | Characteristics of the 1st cycle of pressure wave oscillation in Figure 3

			Protected systems							
			Inline (sub)-short-section				Branching (sub)-short-section			
Parameters		Original system	(HDPE)	(LDPE)	(HDPE/HDPE)	(LDPE/HDPE)	(HDPE	(LDPE)	(HDPE/HDPE)	(LDPE/HDPE)
T_1 (periods)	(s)	0.420	0.756	1.18	0.876	0.612	0.904	0.944	0.904	0.944
H_{max}	(m)	85.6	79.0	66.6	75.4	84.1	80.10	67.60	71.6	80.4
H_{min}	(m)	5.4	15.5	26.1	20.6	20.1	11.40	24.90	22.2	8.2
$\Delta H^+ = H_{max} - H_0$	(m)	40.6	34.0	21.6	30.4	39.1	35.1	22.6	26.6	35.4
$\Delta H^- = H_{min} - H_0$	(m)	39.6	29.5	18.9	24.4	24.9	33.60	20.10	22.8	36.8

shift depicted between the (HDPE/LDPE) branching set-up and the (LDPE) inline or branching set-up is equal to: $\delta''' T_1|^{\text{branching}}_{\text{HDPE}-\text{LDPE}} = |T_1|^{\text{branching}}_{\text{HDPE}-\text{LDPE}} - T_1|^{\text{inline}}_{\text{LDPE}}| = 0.276\,\text{s}$ or $\delta'''' T_1|^{\text{branching}}_{\text{HDPE}-\text{LDPE}} = |T_1|^{\text{branching}}_{\text{HDPE}-\text{LDPE}} - T_1|^{\text{branching}}_{\text{LDPE}}| = 0.262\,\text{s}$, respectively. In other words, the performance index of the (HDPE/LDPE) branching set-up relative to the (LDPE) inline or branching set-up is equal to: $\mu'''^{+}|^{\text{branching}}_{\text{HDPE}-\text{LDPE}} = \{\delta''' H^+|^{\text{branching}}_{\text{HDPE}-\text{LDPE}}/\delta''' T_1|^{\text{inline}}_{\text{LDPE}}\} = 18.11\,\text{ms}^{-1}$ or $\mu''''+|^{\text{branching}}_{\text{HDPE}-\text{LDPE}} = = \{\delta'''' H^+|^{\text{branching}}_{\text{HDPE}-\text{LDPE}}/\delta'''' T_1|^{\text{branching}}_{\text{LDPE}}\} = 15.27\,\text{ms}^{-1}$, respectively.

The second part of this investigation is dedicated to the sensitivity analysis of the first pressure head peak and the period of the first cycle of wave oscillation values, depending on the plastic sub-short-section's diameter and length. This analysis may be achieved based on the variation of the proportion between the (HDPE) and (LDPE) sub-short-sections lengths, maintaining the total length of the two sub-short-sections equal to the primitive value (i.e., 5m); and the diameter of the (HDPE) or (LDPE) sub-short-section only, while the diameter of the second one is maintained at the primitive value: (i.e., 53.2 mm).

For completeness, the forgoing analysis is plotted in Figure 4(a) and 4(b), respectively.

Based on Figure 4(a) and 4(b), it may be concluded that the first pressure head peak and the period of the first cycle of pressure wave oscillation are markedly influenced by the (HDPE) sub-short-section length and diameter; however, there is no appreciable variation of the two former

parameters due to the variation of the (LDPE) sub-short-section length and diameter.

Case 2: Control of negative-surge initiated water hammer waves

The hydraulic system considered here comprises a sloping steel piping system ($L = 100$ m; $D = 53.2$ mm; $e = 3.35$ mm; $a_0 = 1369.7$ m/s and $J_0 = 0.0049$ GPa^{-1}), connecting two pressurized tanks (Figure 5(a)). The downstream pipe axis is taken as the horizontal datum level (i.e., $z_d = 0$ m), and the upstream reservoir level is $z_u = 2.03$ m. The gauge saturated pressure head of the liquid is: $H_g = -10.29$ m. The initial steady-state flow regime is characterized by a constant flow velocity: $V_0 = 0.3$ m/s and a constant pressure head value equal to: $H_0^{T_2} = 21.4$ m, maintained in the downstream pressurized tank. The considered transient is caused by an instantaneous and full closure of the upstream control valve, initiating a negative-surge wave. Such a condition may be written as follows:

$$Q_{|x=0} = 0 \text{ and } H_{|x=L} = H_0^{T_2} \ (t \succ 0) \tag{12}$$

For such a case, the branching or inline strategy based on the dual technique may be implemented as shown in Figure 5(b) or 5(c).

As for the preceding test case, the sub-short-section length and diameter values, associated with the implementation of the dual technique, are first selected equal to: $l_{\text{dual}}^{\text{sub-short-section}} = 5\text{m}$ and $d_{\text{dual}}^{\text{sub-short-section}} (= D) = 53.2\,\text{mm}$, respectively. Therefore, the short-section length and diameter used in the conventional technique, calculated from Equation (10), is: $l_{\text{conventional}}^{\text{short-section}} (= 2 \times l_{\text{dual}}^{\text{sub-short-section}}) = 10\text{m}$ and $d_{\text{conventional}}^{\text{short-section}} (= d_{\text{dual}}^{\text{sub-short-section}}) = 53.2\,\text{mm}$, respectively.

Figures 6 compares the upstream pressure head evolutions, predicted into the non-protected hydraulic system case, alongside their counterparts predicted into the protected system cases using a (HDPE/LDPE) dual technique set-up-based inline or branching strategy and an (HDPE) or (LDPE) conventional technique configuration-based inline or branching strategy. Additionally, Table 2 reports the main features of the pressure waves displayed in Figure 6.

Figure 6 clearly confirms the cavitating flow onset in the non-protected system case, due to the upstream valve closure. For this transient regime, the pressure head oscillation is characterized by large and short duration pulses. For instance, the positive and negative pressure head magnitudes are: $\Delta H^+|_{\text{STEEL}} = 41.8$ m and $\Delta H^-|_{\text{STEEL}} = 32.6$ m, respectively, and the period of the first pressure wave oscillation cycle is equal to: $T_1|_{\text{STEEL}} = 0.472$ s.

Nonetheless, referring to Figure 6, the cavitating flow phenomenon is mitigated in all protected systems' cases.

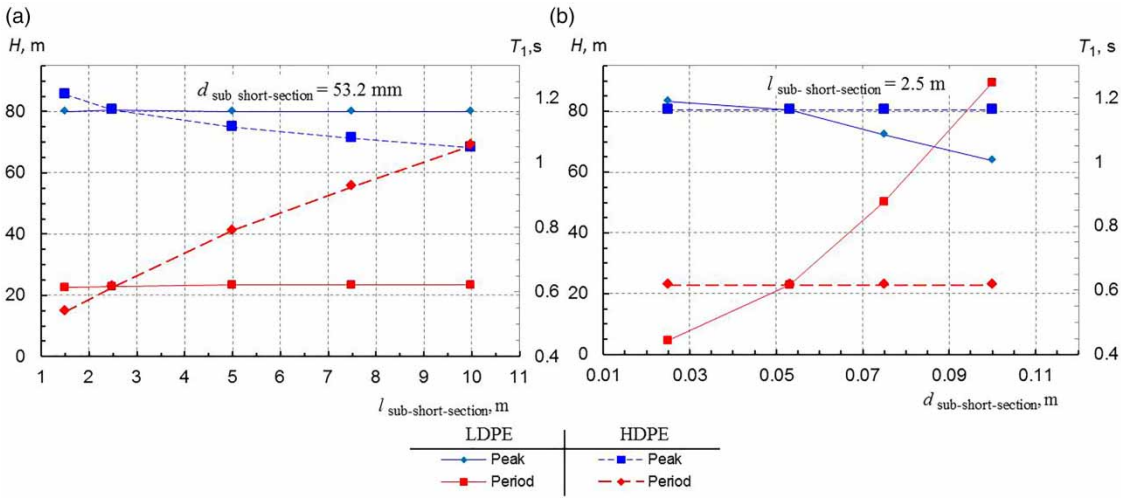

Figure 4 | Sensitivity of the first pressure head peak and the period of the 1st cycle of pressure wave oscillations to the plastic sub-short-sections: (a) lengths (for $d_{\text{sub short-section}} = 53.2$ mm) and (b) diameters (for $l_{\text{sub short-section}} = 2.5$ m), for the (LDPE-HDPE)-branching set-up-based controlled system.

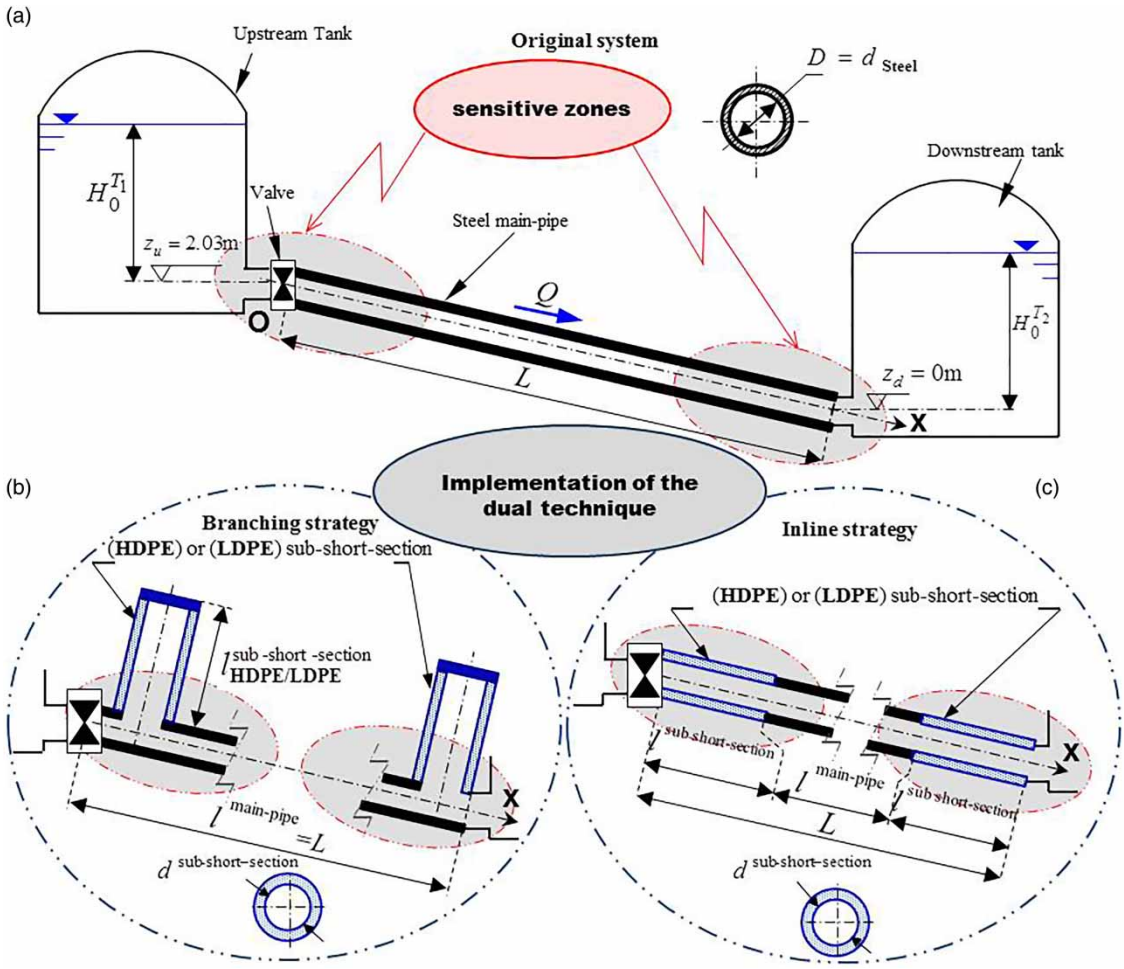

Figure 5 | Sketch of the hydraulic system for the negative-surge control test case: (a) the original system and the controlled system using the dual technique-based (b) branching and (c) inline strategy.

For these cases, the pressure head curves exhibit attenuated positive and negative magnitude values and increasing pressure wave oscillation period values depending on the employed technique (i.e., dual or conventional) and strategy (i.e., inline or branching).

Based on Figure 6 and Table 2, the first pressure head peak and crest performed by the (HDPE/LDPE) branching or inline set-up are almost similar to the first cycle of pressure head oscillation ($\Delta H^{+}|^{\text{branching}}_{\text{HDPE}-\text{LDPE}} = 15.8$ m, $\Delta H^{-}|^{\text{branching}}_{\text{HDPE}-\text{LDPE}} = 32.6$ m and $T_1|^{\text{branching}}_{\text{HDPE}-\text{LDPE}} = 1.36$ s or $\Delta H^{+}|^{\text{inline}}_{\text{HDPE}-\text{LDPE}} = 15.9$ m $\Delta H^{-}|^{\text{inline}}_{\text{HDPE}-\text{LDPE}} = 19.1$ m and $T_1|^{\text{inline}}_{\text{HDPE}-\text{LDPE}} = 1.34$ s, respectively). However, more important discrepancies are observed in the subsequent cycles. For example, the negative-surge magnitude and the period of the 4th pressure head oscillation cycle estimated in the (HDPE/LDPE) branching or inline set-up of the protected system case are: $\Delta H_4^{-}|^{\text{branching}}_{\text{HDPE}-\text{LDPE}} = 13.8$ m and $T_4|^{\text{branching}}_{\text{HDPE}-\text{LDPE}} = 1.35$ s or $\Delta H_4^{-}|^{\text{inline}}_{\text{HDPE}-\text{LDPE}} = 14.5$ m and $T_4|^{\text{inline}}_{\text{HDPE}-\text{LDPE}} = 0.78$ s, respectively. In other words, the ratio between the negative-surge magnitude and the period of the first cycle of pressure head oscillation is: $\{\Delta H^{+}/T_1\}|^{\text{branching}}_{\text{HDPE}-\text{LDPE}} = 10.22\ \text{ms}^{-1}$ or $\{\Delta H^{+}/T_1\}|^{\text{inline}}_{\text{HDPE}-\text{LDPE}} = 18.59\ \text{ms}^{-1}$, corresponding to the (HDPE/LDPE) branching or inline set-up. This, in turn, implies that the (HDPE/LDPE) branching set-up allows better trade-off between pressure head attenuation and pressure wave oscillation period spreading than the (HDPE/LDPE) inline set-up. Thereupon, this specific set-up is next analyzed in detail.

As compared with the original system case, the (HDPE/LDPE) branching set-up provides important attenuation of

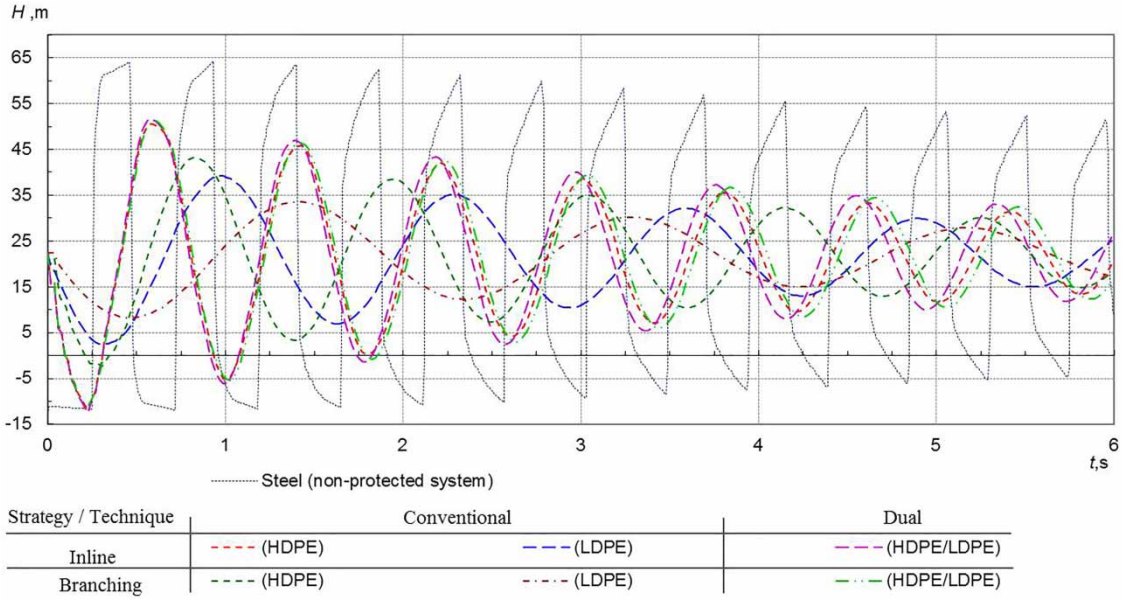

Figure 6 | Upstream pressure head signals for the non-protected and protected systems based on the dual and conventional techniques.

Table 2 | Characteristics of the 1st cycle of pressure wave oscillation in Figure 6

			Protected systems							
			Inline (sub)-short-section				Branching (sub)-short-section			
Parameters		Original system	(HDPE)	(LDPE)	(HDPE/HDPE)	(LDPE/HDPE)	(HDPE	(LDPE)	(HDPE/HDPE)	(LDPE/HDPE)
T_1 (periods)	(s)	0.472	0.798	1.31	0.798	1.340	0.748	1.166	0.798	1.360
H_{max}	(m)	64.2	50.2	38.9	51.3	38.3	43.2	49.7	51.3	38.2
H_{min}	(m)	−10.2	−10.2	2.8	−10.2	3.3	−2.4	−9.9	−10.2	3.3
$\Delta H^+ = H_{max} - H_0$	(m)	41.8	27.9	16.5	29.0	16.0	20.8	27.3	29.0	15.9
$\Delta H^- = H_{min} - H_0$	(m)	32.6	32.6	19.6	32.6	19.0	24.8	32.3	32.6	19.0

first pressure head crest: $\delta H^-|^{branching}_{HDPE-LDPE} = |\Delta H^-|^{branching}_{HDPE-LDPE} - \Delta H^-|_{STEEL}| = 13.5$ m. However, this set-up induces a longer pressure wave oscillation period as compared with the original system case. Specifically, the phase shift depicted between the (HDPE/LDPE) branching set-up and the original system case is equal to: $\delta T_1|^{branching}_{HDPE-LDPE} = |T_1|^{branching}_{HDPE-LDPE} - T_1|_{STEEL}| = 0.889$ s. In other words, the performance index of the (HDPE/LDPE) branching set-up relative to the original system case is equal to: $\mu^-|^{branching}_{HDPE-LDPE} = \{\delta H^-|^{branching}_{HDPE-LDPE}/\delta T_1|_{STEEL}\} = 15.185\ ms^{-1}$.

Similarly, the (HDPE/LDPE) inline set-up provides more important attenuation of first pressure head peak as compared with the (HDPE) inline or branching set-up: $\delta' H^-|^{branching}_{HDPE-LDPE} = |\Delta H^-|^{branching}_{HDPE-LDPE} - \Delta H^-|^{inline}_{HDPE}| = 26.9$ m or $\delta'' H^-|^{branching}_{HDPE-LDPE} = |\Delta H^-|^{branching}_{HDPE-LDPE} - \Delta H^-|^{branching}_{HDPE}| = 13.9$ m, respectively. However, this set-up induces a longer pressure wave oscillation period compared with the original system case. Specifically, the phase-shift depicted between the (HDPE/LDPE) inline set-up and the (HDPE) inline or branching set-up is equal to: $\delta' T_1|^{branching}_{HDPE-LDPE} = |T'_1|^{branching}_{HDPE-LDPE} - T'_1|^{inline}_{HDPE}| = 0.374$ s or $\delta'' T_1|^{branching}_{HDPE-LDPE} = |T''_1|^{branching}_{HDPE-LDPE} - T''_1|^{branching}_{HDPE}| = 0.562$ s, respectively. In other words, the performance index of the (HDPE/LDPE) inline set-up relative to the (HDPE) inline or branching set-up is equal to: $\mu'|^{branching}_{HDPE-LDPE} = \{\delta' H^-|^{branching}_{HDPE-LDPE}/\delta' T_1|^{branching}_{HDPE-LDPE}\} = 30\ ms^{-1}$, or $\mu''-|^{branching}_{HDPE-LDPE} = \{\delta'' H^-|^{branching}_{HDPE-LDPE}/\delta'' T_1|^{branching}_{HDPE-LDPE}\} = 50.47\ ms^{-1}$, respectively.

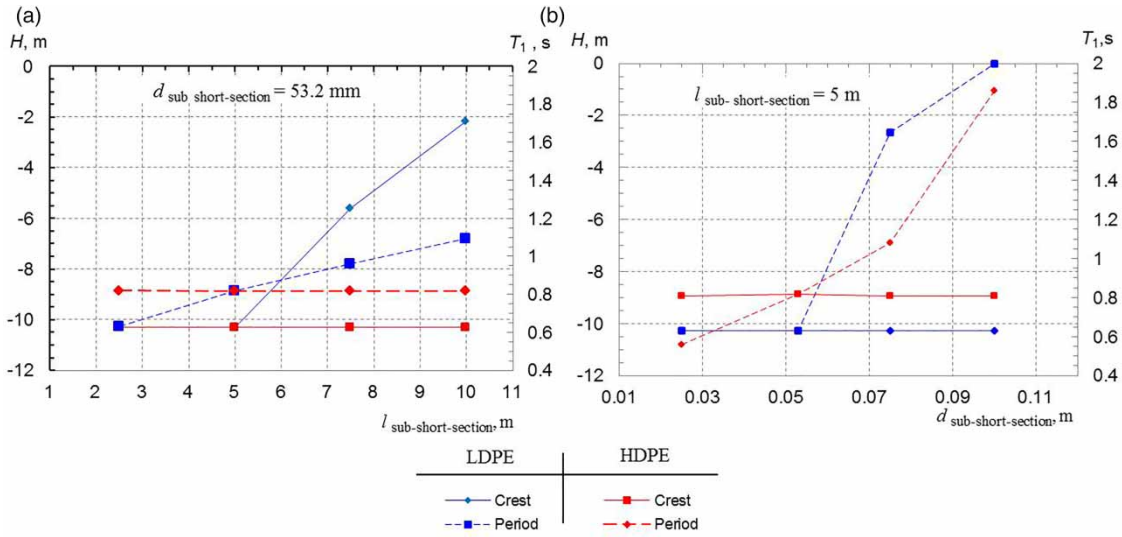

Figure 7 | Sensitivity of the first pressure head crest and the period of the 1st cycle of pressure wave oscillations to the plastic sub-short-sections: (a) lengths (for $d_{\text{sub short-section}} = 53.2$ mm) and (b) diameters (for $l_{\text{sub short-section}} = 5$ m), for the (LDPE-HDPE)-branching set-up-based controlled system.

Contrarily, the (HDPE/LDPE) inline set-up provides less important attenuation of first pressure head peak as compared with the (LDPE) inline or branching set-up: $\delta''' H^- |^{\text{branching}}_{\text{HDPE}-\text{LDPE}} = \Delta H^- |^{\text{branching}}_{\text{HDPE}-\text{LDPE}} - \Delta H^- |^{\text{inline}}_{\text{LDPE}} = 0.5$ m or $\delta'''' H^- |^{\text{branching}}_{\text{HDPE}-\text{LDPE}} = |\Delta H^- |^{\text{branching}}_{\text{HDPE}-\text{LDPE}} - \Delta H^- |^{\text{branching}}_{\text{LDPE}}| = 13.2$ m, respectively. In addition, this set-up induces lesser pressure wave oscillation period as compared with the (LDPE) inline or branching set-up. Specifically, the phase-shift depicted between the former and latter set-ups is equal to: $\delta''' T_1 |^{\text{branching}}_{\text{HDPE}-\text{LDPE}} = |T_1 |^{\text{branching}}_{\text{HDPE}-\text{LDPE}} - T_1 |^{\text{inline}}_{\text{LDPE}}| = 0.05$ s or $\delta'''' T_1 |^{\text{branching}}_{\text{HDPE}-\text{LDPE}} = |T_1 |^{\text{branching}}_{\text{HDPE}-\text{LDPE}} - T_1 |^{\text{branching}}_{\text{LDPE}}| = 0.515$ s, respectively. In other words, the performance index of the (HDPE/LDPE) inline set-up relative to the (HDPE) inline or branching set-up is equal to: $\mu''' |^{\text{branching}}_{\text{HDPE}-\text{LDPE}} = \{\delta''' H^- |^{\text{branching}}_{\text{HDPE}-\text{LDPE}} / \delta''' T_1 |^{\text{inline}}_{\text{HDPE}}\} = 0.1$ ms^{-1} or $\mu'''' |^{\text{branching}}_{\text{HDPE}-\text{LDPE}} = \{\delta'''' H^- |^{\text{branching}}_{\text{HDPE}-\text{LDPE}} / \delta'''' T_1 |^{\text{branching}}_{\text{HDPE}}\} = 25.63$ ms^{-1}, respectively.

The second part of this study is devoted to the sensitivity analysis of the first pressure head peak value and the period of the first cycle of pressure wave oscillation, depending on the plastic sub-short-section diameters and lengths. This analysis may be achieved based on the variation of the proportion between the (HDPE) and (LDPE) sub-short-section lengths, maintaining the total length of the two sub-short-sections equal to the primitive value (i.e., 5m); and the variation of the diameter of the (HDPE) or (LDPE) sub-short-section only, while maintaining the diameter of the second one equal to its primitive value: (i.e., 53.2 mm).

For completeness, the forgoing analysis is plotted in Figures 7(a) and 7(b), respectively.

Based on Figures 7(a) and 7(b), it may be concluded that the first pressure head crest and the period of the first cycle of pressure wave oscillation are mainly influenced by the (HDPE) sub-short-section length and diameter; however, there is no appreciable variation of the two former parameters due to the variation of the (LDPE) sub-short-section length and diameter.

CONCLUSIONS

Overall, the findings proved that the conjunctive use of two sub-short-sections could improve the conventional technique-based inline or branching strategy with regard to attenuation of pressure head peak and crest; while limiting excessive spreading of pressure wave oscillation period. Along these lines, it was demonstrated that the better trade-off between the two latter effects was obtained for the (HDPE/LDPE) dual technique-based branching strategy, (where the former sub-short-section is attached to the sensitive region of the steel piping system parts, while the latter is attached to the second steel piping system extremity). In addition, it was also found that the pressure head peak (or

crest) and the pressure wave oscillation period values were markedly sensitive to the (HDPE) sub-short-section.

Ultimately, the findings proved that the proposed innovative dual technique is a useful design tool for upgrading existing steel piping systems facing both positive and negative surge water hammer severe effects, while providing inherently free maintenance and/or testing merits compared with classical surge control devices.

REFERENCES

Aklonis, J. J., MacKnight, W. J. & Shen, M. 1972 *Introduction to Polymer Viscoelasticity*. Wiley-Interscience, NewYork, USA.

Bergant, A. & Simpson, A. 1999 Pipeline column separation flow regimes. *J. Hydraul. Eng. ASCE* **125**, 835–848.

Besharat, M., Tarinejad, R. & Ramos, H. 2015 The effect of water hammer on a confined air pocket towards flow energy storage system. *J. Water Supply Res. Technol.-Aqua* **65** (2), 116–126. doi:10.2166/aqua.2015.081.

Covas, D., Stoianov, I., Ramos, H., Graham, N., Maksimovic, C. & Butler, D. 2004 Waterhammer in pressurized polyethylene pipes: conceptual model and experimental analysis. *Urban Water J.* **1** (2), 177–197.

Deyou, L., Xiaolong, F., Zhigang, Z., Hongjie, W., Zhenggui, L., Shuhong, L. & Xianzhu, W. 2019 Investigation methods for analysis of transient phenomena concerning design and operation of hydraulic-machine systems – A review. *Renew. Sust Energ Rev.* **101**, 26–46. doi: 10.1016/j.rser.2018.10.023.

Ferry, J. D. 1970 *Viscoelastic Properties of Polymers*, 2nd ed. John Wiley & Sons, New York, USA.

Fersi, M. & Triki, A. 2019a Investigation on re-designing strategies for water-hammer control in pressurized-piping systems. *J. Press. Vessel Technol.* **141** (2). doi: 10.1115/1.4040136.

Fersi, M. & Triki, A. 2019b Alternative design strategy for water-hammer control in pressurized-pipe flow. In: *Advances in Acoustics and Vibration II. ICAV 2018 Applied Condition Monitoring*, Vol. 13 (T. Fakhfakh, C. Karra, S. Bouaziz, F. Chaari & M. Haddar, eds). Springer, Cham, Switzerland, pp. 157–165. doi:10.1007/978-3-319-94616-0_16.

Gally, M., Guney, M. & Rieutford, E. 1979 An investigation of pressure transients in viscoelastic pipes. *J. Fluid Eng. Trans. ASME* **101**, 495–499.

Ghilardi, P. & Paoletti, A. 1986 Additional viscoelastic pipes as pressure surge suppressors. In: *Proceedings of 5th International Conference on Pressure Surges*, Hannover, Germany, pp. 113–121.

Keramat, A. & Haghighi, A. 2014 Straightforward transient-based approach for the creep function determination in viscoelastic pipes. *J. Hydraul. Eng.* **140** (12), 04014058. https://doi.org/10.1061/(ASCE)HY.1943-7900.0000929.

Lamaddalena, N., Khadra, R., Derardja, B. & Fratino, U. 2018 A new indicator for unsteady flow analysis in pressurized irrigation systems. *Water Resour. Manage.* **9**. doi.:10.1007/s11269-018-1987-4.

Liao, S., Zhao, H., Li, G. & Liu, B. 2019 Short-term load dispatching method for a diversion hydropower plant with multiple turbines in one tunnel using a two-stage model. *Energies*. **12** (8), 1476. doi:10.3390/en12081476.

Massouh, F. & Comolet, R. 1984 Étude d'un système anti-bélier en ligne. (Study of a water-hammer protection system in line). *La Houille Blanche* **5**, 355–362.

Pezzinga, G. & Scandura, P. 1995 Unsteady flow in installations with polymeric additional pipe. *J. Hydraul. Eng. ASCE* **121** (11), 802–811. doi.:10.1061/(ASCE)0733-9429(1995)121:11(802).

Trabelsi, M. & Triki, A. 2019 Dual control technique for mitigating water-hammer phenomenon in pressurized steel-piping systems. *Int. J. Pressure Vessels Piping* **172**, 379–413. doi:10.1016/j.ijpvp.2019.04.011.

Triki, A. 2016 Water-hammer control in pressurized-pipe flow using an in-line polymeric short-section. *Acta Mechanica* **227** (3), 777–793. doi:10.1007/s00707-015-1493-13.

Triki, A. 2017 Water-hammer control in pressurized-pipe flow using a branched polymeric penstock. *J. Pipeline Syst. Eng. Pract. ASCE* **8** (4), 04017024. doi:10.1061/(ASCE)PS.1949- 1204.0000277.

Triki, A. 2018a Further investigation on water-hammer control inline strategy in water-supply systems. *J. Water Supply Res. Technol.-AQUA* **67** (1), 30–43. doi:10.2166/aqua.2017.073.

Triki, A. 2018b Dual-technique based inline design strategy for water-hammer control in pressurized-pipe flow. *Acta Mechanica* **227** (3), 777–793. doi:10.1007/s00707-017-2085-z.

Triki, A. & Chaker, M. A. 2019 Compound technique-based inline design strategy for water-hammer control in steel pressurized-piping systems. *Int. J. Pressure Vessels Piping* **169**, 188–203. doi:10.1016/j.ijpvp.2018.12.001.

Triki, A. & Fersi, M. 2018 Further investigation on the water-hammer control branching strategy in pressurized steel-piping systems. *Int. J. Pressure Vessels Piping* **165**, 135–144. doi:10.1016/j.ijpvp.2018.06.002.

Vitkovsky, J. P., Lambert, M. F., Simpson, A. R. & Bergant, A. 2000 Advances in unsteady friction modelling in transient pipe flow. In: *8th International Conference on Pressure Surges, BHR*, The Hague, the Netherlands.

Wan, W. & Zhang, B. 2018 Investigation of water hammer protection in water supply pipeline systems using an intelligent self-controlled surge tank. *Energies* **11** (6), 1450. doi:10.3390/en11061450.

Wylie, E. B. & Streeter, V. L. 1993 *Fluid Transients in Systems*. Prentice Hall, Englewood Cliffs, NJ, USA.

Yuzhanin, V., Popadko, V., Koturbash, T., Chernova, V. & Barashkin, R. 2019 Predictive control and suppression of pressure surges in main oil pipelines with counter-running pressure waves. *Int. J. Pressure Vessels Piping* **172**, 2–47. doi:10.1016/j.ijpvp.2019.03.015.

First received 22 January 2019; accepted in revised form 1 May 2019. Available online 21 June 2019